

Noisy Coherent Population Trapping: Applications to Noise Estimation and Qubit State Preparation

Arshag Danageozian,* Nathaniel R. Miller, Pratik J. Barge, Narayan Bhusal, and Jonathan P. Dowling[†]

*Hearne Institute for Theoretical Physics and Department of Physics & Astronomy,
Louisiana State University, Baton Rouge, LA 70803, USA*

(Dated: March 1, 2025)

Coherent population trapping is a well-known quantum phenomenon in a driven Λ system, with many applications across quantum optics. However, when a stochastic bath is present in addition to vacuum noise, the observed trapping is no longer perfect. Here we derive a time-convolutionless master equation describing the equilibration of the Λ system in the presence of additional temporally correlated classical noise, with an unknown decay parameter. Our simulations show a one-to-one correspondence between the decay parameter and the depth of the characteristic dip in the photoluminescence spectrum, thereby enabling the unknown parameter to be estimated from the observed spectra. We apply our analysis to the problem of qubit state initialization in a Λ system via dark states and show how the stochastic bath affects the fidelity of such initialization as a function of the desired dark-state amplitudes. We show that an optimum choice of Rabi frequencies is possible.

I. INTRODUCTION

Coherent population trapping (CPT) [1–4] is a quantum mechanical phenomenon in driven three-level Λ systems used to make a specific material transparent to certain frequencies. Under appropriate driving conditions, the dynamics of the Λ system gets “trapped” into the Hilbert subspace of the two ground levels, in a coherent superposition which can no longer absorb the light. Such a superposition is known as a “dark state,” because it is no longer coupled to the excited state and fluorescent light emission is then suppressed. Under current advances in quantum control, applications of CPT have attracted growing interest outside the field of optics. In the context of dissipative quantum state preparation [5–10], this concept is used to stabilize arbitrary linear superpositions of two ground states by driving the Λ system into the (unique) dark state, with the amplitudes of the superposition being determined by the ratio between the two Rabi frequencies and the relative phase between the two laser fields. Notably, CPT plays an important role in protocols for all-optical manipulations in nitrogen-vacancy (NV) centers in diamond [11–14]. More recently, CPT has found application in real-time quantum sensing, by allowing the effective magnetic field in a medium to be estimated via the rate of photon counts under CPT conditions [15].

Currently, standard theoretical analyses of CPT only account for decoherence due to the quantum vacuum [2, 16, 17]. However, this need not be the only source of noise in many realistic settings of interest. Even assuming that any operational source of noise (e.g., control amplitude or frequency fluctuations) may be experimentally minimized, it is important to expand the treatment to include noise arising directly from the hosting medium

in which the Λ system is implemented. While we can argue for a noise model that is specific for each medium (environment) on physical grounds, the resulting functional forms will typically still have unknown (e.g., decay) noise parameters that need to be estimated from experimentally accessible quantities.

In this work, after describing the physical setting in Sec. II, we theoretically analyze the CPT dynamics of a general Λ system under the simultaneous presence of vacuum noise and noise due a classical stochastic environment (Sec. III). Our approach is based on deriving an appropriate time-convolutionless (TCL) master equation (ME) [18]. Based on our analysis, we first show (Sec. IV A) a correspondence between the height of the dip in the CPT photoluminescence spectrum and the unknown decay parameter of the classical environment, thereby enabling an estimation of this parameter from observed spectra. In Sec. IV B, we further apply this result to quantify the fidelity loss that the noise induces in CPT-based dissipative state initialization, as considered in [7]. Thus, in our analysis, CPT serves two different but complementary purposes: decay parameter estimation and dissipative state preparation.

While our theoretical approach may be applied to an arbitrary Λ system in principle, we use the NV center [19–21] as a realistic illustrative setting for our analysis. NV centers are highly studied solid-state systems due to both their long qubit coherence times (ranging from 10^{-6} s to 10^{-3} s depending on the isotopic purity of the diamond sample [22–24]) and their dynamic accessibility for initialization and read-out using optical pulses. Furthermore, they are scalable solid-state systems [25], which makes them a good candidate for various quantum technology applications.

II. PHYSICAL SETTING

The NV center is embedded in diamond, which is composed mostly of ^{12}C isotopes (see Fig.(1a)). However, a

* Corresponding Author: arshag.danageozian@gmail.com

[†] Deceased, June 5 2020.

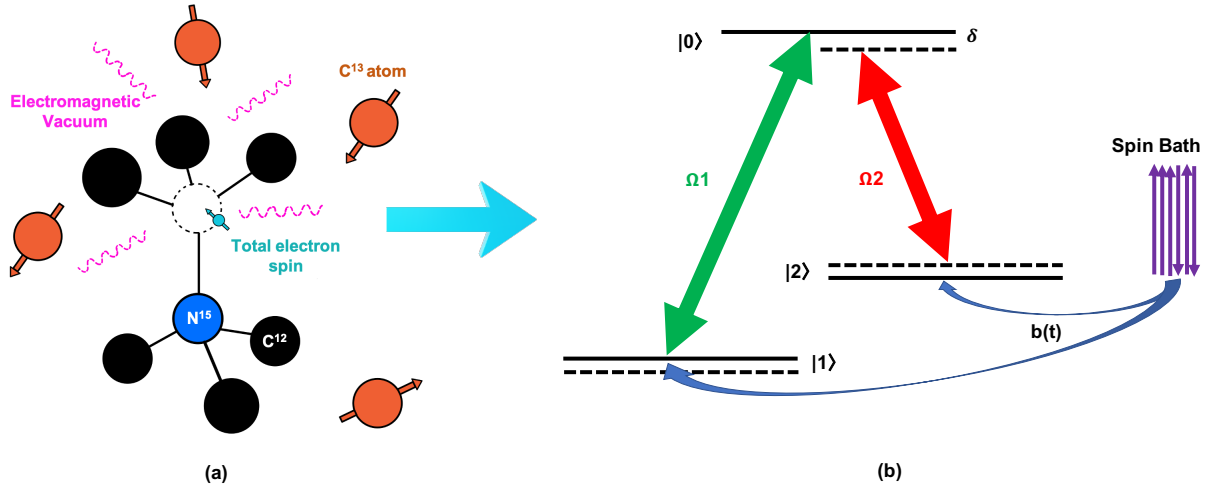


FIG. 1. (Color online) (a) Schematic of an NV center in the diamond lattice. Both the ^{13}C nuclear spin bath and the quantum vacuum are explicitly shown. (b) Qualitative diagram of the energy levels and couplings of the selected Λ system to two coherent light sources (solid green and dashed red) and the nuclear spin bath.

small portion of the Carbon atoms (about 1.1% in common samples) are ^{13}C . Since the latter is the only one that has a non-zero nuclear spin ($I = 1/2$), it is the one that couples to the electronic spin degrees of freedom of the NV center. Using two coherent light sources, the NV center is driven to be an effective Λ system [12–14, 16, 17, 26]. In an ideal scenario, no photons are emitted when CPT is achieved. However, in the presence of noise, the expected value of the excited state population in CPT becomes larger than zero, and additional photons are emitted [13].

Throughout our analysis, we assume the quantization axis to be along the NV center axis. It is well known that the NV center satisfies the C_{3v} point-group symmetry; hence we shall use the corresponding group-theoretical notation. For the excited state of the Λ system [20, 27–29], we choose the state A_2 , motivated by the fact that it does not couple strongly to the non-radiative singlet states [30]. Combined with the two $m_s = \pm 1$ ground states $\{^3A_{2(-)}, ^3A_{2(+)}\}$, this gives us a nearly perfectly closed Λ system, which has already been demonstrated experimentally [13, 31, 32]. We denote the states A_2 , $^3A_{2(-)}$, $^3A_{2(+)}$ by $|0\rangle$, $|1\rangle$, and $|2\rangle$, respectively (see Fig. 1(b)). We also make the tensor product between the orbital and spin degrees of freedom of the electronic structure explicit, by letting

$$\begin{aligned} |0\rangle &\equiv |A_2\rangle = |E_-\rangle \otimes |+1\rangle + |E_+\rangle \otimes |-1\rangle, \\ |1\rangle &\equiv |^3A_{2(+)}\rangle = |E_0\rangle \otimes |+1\rangle, \\ |2\rangle &\equiv |^3A_{2(-)}\rangle = |E_0\rangle \otimes |-1\rangle. \end{aligned} \quad (1)$$

Here, $|E_0\rangle$ and $|E_{\pm}\rangle$ are the orbital angular momentum eigenstates of the NV-center electron system [28], labelled by eigenvalues 0 and ± 1 of $L_z^{(e)}$. The $|\pm 1\rangle$ states denote the two spin angular momentum eigenstates, la-

belled by the eigenvalues of $S_z^{(e)}$.

The Hamiltonian of the driven Λ system is given by $H_{\Lambda}(t) \equiv H_{\Lambda}^0 + H_{\text{drive}}(t)$ where, by assuming units $\hbar = 1$, the two contributions take the form

$$\begin{aligned} H_{\Lambda}^0 &= \omega_0|0\rangle\langle 0| + \omega_1|1\rangle\langle 1| + \omega_2|2\rangle\langle 2|, \\ H_{\text{drive}}(t) &= (\Omega_1/2)e^{-i(\omega_{L1}t+\phi_1)}|1\rangle\langle 0| \\ &\quad + (\Omega_2/2)e^{-i(\omega_{L2}t+\phi_2)}|2\rangle\langle 0| + \text{H.c.}, \end{aligned} \quad (2)$$

where Ω_1 and Ω_2 are the Rabi frequencies, and (ω_{L1}, ϕ_1) and (ω_{L2}, ϕ_2) the frequencies and phases of the two coherent light sources, respectively. As mentioned in the introduction, we shall work under the assumption that any control errors arising in the implementation of $H_{\text{drive}}(t)$ may be neglected in comparison with environmental noise.

We model the effect of the ^{13}C nuclear-spin bath [33] on the Λ system as a fluctuating classical magnetic field. The value of this field at the position of the NV center at time t is denoted by $b(t)$. Specifically, we assume the spin-bath noise to be zero-mean, stationary, and sufficiently weak to be treated perturbatively (see Sec. III B). In particular, the lowest-order (two-point) correlation function is determined by

$$C(t_1, t_2) \equiv \mathbb{E}\{b(t_1)b(t_2)\} = C(|t_1 - t_2|), \quad (3)$$

where \mathbb{E} denotes the ensemble average over realizations of the classical stochastic process $\{b(t)\}$. In the presence of this stochastic bath, the Hamiltonian of the driven Λ system is then given by $H(t) \equiv H_{\Lambda}(t) + H_c(t)$, where

$$H_c(t) \equiv H_c[b(t)] = -\mu_B(L_z^{(e)} + 2S_z^{(e)})b(t), \quad (4)$$

is the semi-classical interaction Hamiltonian describing the coupling of the electronic system to the field, with $\mu_B = \frac{e\hbar}{2m_e c}$ being the Bohr magneton. We write such a

Hamiltonian in the Λ -system basis of Eqs. (1) as

$$H_c(t) = \sum_{i,j=0,1,2} \langle i | H_c(t) | j \rangle |i\rangle\langle j|.$$

Using the fact that the expectation value of the operators $L_z^{(e)}$ and $S_z^{(e)}$ are given by $(0,0)$, $(0,1)$, and $(0,-1)$ for the states $|0\rangle$, $|1\rangle$, and $|2\rangle$, respectively, along with the orthonormality of the states $|E_0\rangle$ and $|E_{\pm}\rangle$, we arrive at

$$H_c(t) = -\gamma_e b(t) |1\rangle\langle 1| + \gamma_e b(t) |2\rangle\langle 2|, \quad (5)$$

where $\gamma_e = \frac{e\hbar}{m_e c}$ is the gyromagnetic ratio of the electron. Physically, $\gamma_e b(t)$ is the time-dependent frequency fluctuation of the Λ -system ground states; see Fig. 1(b).

III. NOISY COHERENT POPULATION TRAPPING

A. Master equation for ideal CPT dynamics

As mentioned, CPT is an equilibration phenomenon in a driven three-level Λ system where, irrespective of the initial state [6, 34], the dynamics gets restricted to the two-ground-state manifold. Physically, this is a quantum-mechanical consequence of the destructive interference between the two transition probability amplitudes from individual ground states to the same excited state in the Λ system. In order to set the stage for the noisy setting, we briefly review the derivation of a quantitative model within a ME formalism.

In the presence of spontaneous decay alone, the system and the bath are described by the total Hamiltonian

$$H_{\text{tot}}^0(t) \equiv H_{\Lambda}^0 + H_{\text{drive}}(t) + H_{\text{vac}} + H_{\Lambda\text{-vac}}, \quad (6)$$

where H_{vac} is the Hamiltonian of the electromagnetic vacuum and $H_{\Lambda\text{-vac}}$ is the interaction Hamiltonian between the Λ system and the vacuum, in the standard dipole approximation. We write the ME in the interaction picture with respect to $H_{\Lambda}^0 + H_{\text{vac}}$ and denote an operator X in this representation by \tilde{X} . The Liouville-von Neumann equation describing the evolution of the driven Λ system and the vacuum is then given by

$$\dot{\tilde{\sigma}}(t) = -i[\tilde{H}_{\text{drive}}(t) + \tilde{H}_{\Lambda\text{-vac}}(t), \tilde{\sigma}(t)],$$

where $\tilde{\sigma}(t)$ is the density matrix of the total system. By assuming that the joint initial state $\sigma(0) = \rho(0) \otimes \rho_{\text{vac}}$ is product, and treating the coupling to the vacuum in the standard Born-Markov approximation [18], the resulting reduced dynamics is given by a Lindblad ME of the form

$$\frac{d}{dt} \text{Tr}_{\text{vac}} \tilde{\sigma}(t) = \dot{\tilde{\rho}}(t) = -i[\tilde{H}_{\text{drive}}(t), \tilde{\rho}(t)] + R_q[\tilde{\rho}(t)], \quad (7)$$

where the Hamiltonian may be explicitly computed from

Eq. (2) and

$$R_q[\tilde{\rho}] \equiv -\frac{1}{2} \sum_{i=1,2} (L_i^\dagger L_i \tilde{\rho} + \tilde{\rho} L_i^\dagger L_i - 2L_i \tilde{\rho} L_i^\dagger) \quad (8)$$

is the dissipator accounting for the quantum Markovian environment. The two Lindblad operators are given by

$$L_i = \sqrt{\Gamma/2} |i\rangle\langle 0|, \quad \text{for } i = \{1, 2\}, \quad (9)$$

where $\Gamma = \Gamma_{01} \approx \Gamma_{02}$ is the decay rate from the excited state to each of the ground states (explicitly, $\Gamma_{0i} = (\omega_0 - \omega_i)^3 d_{0i}^2 / 3\pi\epsilon_0\hbar c^3$, $i = 1, 2$, where d_{0i} is a matrix element from the dipole coupling matrix [18]). By dropping, for simplicity, the tilde notation for interaction-picture operators, the result is a coupled set of differential equations for the density matrix elements. In particular, in the relevant case where the detunings of the two lasers are $\delta_1 \equiv \delta$ and $\delta_2 = 0$, and $\phi_1 = \phi_2 = 0$, we recover the known expressions (see, for instance, [35]):

$$\begin{aligned} \dot{\rho}_{00} &= -\Gamma\rho_{00} + i\Omega_1/2\rho_{01} + i\Omega_2/2\rho_{02} + c.c., \\ \dot{\rho}_{11} &= \Gamma/2\rho_{00} - i\Omega_1/2\rho_{01} + c.c., \\ \dot{\rho}_{22} &= \Gamma/2\rho_{00} - i\Omega_2/2\rho_{02} + c.c., \\ \dot{\rho}_{01} &= -\Gamma/2\rho_{01} + i\Omega_1/2(\rho_{00} - \rho_{11}) - i\Omega_2/2\rho_{21}, \\ \dot{\rho}_{02} &= (-\Gamma/2 + i\delta)\rho_{02} + i\Omega_2/2(\rho_{00} - \rho_{22}) - i\Omega_1/2\rho_{12}, \\ \dot{\rho}_{12} &= i\delta\rho_{12} - i\Omega_2/2\rho_{02} + i\Omega_1/2\rho_{10}. \end{aligned}$$

The above set of coupled differential equations can be compactly represented in matrix form as

$$\dot{\vec{\rho}} = \hat{A}\vec{\rho}, \quad \vec{\rho} \equiv (\rho_{00}, \rho_{01}, \dots, \rho_{22}), \quad (10)$$

in terms of the vectorized density matrix.

It is well known that for a Lindblad ME as in Eq. (7), a steady-state solution always exists, and it is globally attractive if and only if it is unique [36]. Numerically, we have explicitly verified that $\det \hat{A} = 0$ for arbitrary values of the parameters $\Gamma, \Omega_1, \Omega_2$, and δ . In particular, this implies that the experimentally tunable parameter δ can be varied freely and there will be a steady state $\vec{\rho}_{\delta}^{\text{eq}}$, determined by $\hat{A}\vec{\rho}_{\delta}^{\text{eq}} = 0$. Unsurprisingly, the steady state corresponding to $\delta = 0$ is the dark state

$$|d\rangle \equiv \frac{\Omega_2}{\Omega} |1\rangle - \frac{\Omega_1}{\Omega} |2\rangle, \quad \Omega \equiv \sqrt{\Omega_1^2 + \Omega_2^2},$$

because the CPT condition of having a zero two-photon detuning $\delta_{12} = \delta_1 - \delta_2$ is equivalent to having $\delta = 0$. By invoking the sufficient conditions for uniqueness provided in [36], one may verify that the Lindblad dynamics has the unique steady state $\vec{\rho}_0^{\text{eq}} = |d\rangle\langle d|$ independent of Γ , provided that $\Gamma \neq 0$, in which case this steady state is reached from an arbitrary initial preparation.

B. Master equation for noisy CPT dynamics

Stochastic bath models have been extensively discussed in the literature [18, 37–39]. In the present setting, to integrate the coupling to a quantum (vacuum) environment and to the classical nuclear spin-bath environment into a single equation for the reduced dynamics of the Λ system, we start from the full stochastic Hamiltonian

$$H_{\text{tot}}(t) = H_{\text{tot}}^0(t) + H_c[b(t)],$$

where the noiseless Hamiltonian and the noise term are given by Eqs.(6) and (4), respectively. Moving to the interaction picture with respect to the total free Hamiltonian $H_{\Lambda}^0 + H_{\text{vac}}$, and denoting the full density matrix for a single realization of the stochastic process $\{b(t)\}_t$ by $\sigma(t; \{b(t)\})$, the formal solution of the Liouville-von Neumann equation reads

$$\sigma(t; \{b(t)\}) = \mathcal{T} \exp \left\{ \int_0^t ds \hat{L}(s) \right\} \sigma(0),$$

where \hat{L} is the Liouvillian superoperator corresponding to the interaction part of $H_{\text{tot}}(t)$ in the interaction picture and \mathcal{T} denotes time ordering. Let us define the projection superoperator \hat{P} by requiring that $\hat{P}\sigma \equiv (\text{Tr}_B\sigma) \otimes \rho_B$, for arbitrary σ and fixed ρ_B (the latter is usually taken to be the stationary Gibbs state of the quantum bath) [18]. Assuming as before that $\sigma(0) = \rho(0) \otimes \rho_B$, we get $\hat{P}\sigma(0) = \sigma(0)$. From here on, we shall use van Kampen’s cumulant notation (that is, $\langle \hat{\chi} \rangle = \hat{P}\hat{\chi}\hat{P}$). We apply the projection operator to both sides of the previous equation and use the property $\hat{P}^2 = \hat{P}$ to get

$$\rho(t; \{b(t)\}) \otimes \rho_B = \langle \mathcal{T} \exp \left\{ \int_0^t ds \hat{L}(s) \right\} \rangle \hat{P}\sigma(0).$$

Unlike in the ideal case, notice that we cannot immediately differentiate this equation to obtain a ME because the Liouvillian now depends on a stochastic process $b(t)$ which is everywhere continuous but nowhere differentiable. We average both sides of this equation with respect to the classical noise first and then follow steps that are well known, due to van Kampen [40]. Starting from the ensemble-averaged equation

$$\mathbb{E}(\hat{P}\sigma(t)) = \mathbb{E} \left\{ \langle \mathcal{T} \exp \left\{ \int_0^t ds \hat{L}(s) \right\} \rangle \right\} \hat{P}\sigma(0), \quad (11)$$

we expand the right hand-side to

$$(I + E_0(\hat{1}) + E_0(\hat{1}, \hat{2}) + \dots) \hat{P}\sigma(0),$$

where $E_0(\hat{1}, \hat{2}, \dots, \hat{n})$ is the n -th term in the Dyson expansion, given by

$$\int_0^t dt_n \int_0^{t_n} dt_{n-1} \dots \int_0^{t_2} dt_1 \mathbb{E} \left\{ \langle \hat{L}(t_n) \dots \hat{L}(t_2) \hat{L}(t_1) \rangle \right\}.$$

On the other hand, differentiating Eq. (11) yields

$$\frac{d}{dt} \mathbb{E}(\hat{P}\sigma(t; \{b(t)\})) = (E_1(\hat{1}) + E_1(\hat{1}, \hat{2}) + \dots) \hat{P}\sigma(0), \quad (12)$$

where $E_1(\hat{1}, \hat{2}, \dots, \hat{n})$ denotes the time derivative of $E_0(\hat{1}, \hat{2}, \dots, \hat{n})$. We can rewrite the right hand-side of Eq. (12) in terms of $\mathbb{E}(\hat{P}\sigma(t)) \equiv \sigma_{\text{av}}(t)$ by solving Eq. (11) with respect to $\hat{P}\sigma(0)$ as

$$\hat{P}\sigma(0) = \{1 + E_0(\hat{1}) + E_0(\hat{1}, \hat{2}) + \dots\}^{-1} \sigma_{\text{av}}(t).$$

Upon substituting the result back into Eq. (12), we obtain the TCL ME, $\dot{\sigma}_{\text{av}}(t) = \hat{\kappa}(t)\sigma_{\text{av}}(t)$. The TCL generator $\hat{\kappa}(t)$ is determined in terms of the (van Kampen) cumulants of the Liouvillian superoperator as [18]

$$\{E_1(\hat{1}) + E_1(\hat{1}, \hat{2}) + \dots\} \{1 + E_0(\hat{1}) + E_0(\hat{1}, \hat{2}) + \dots\}^{-1},$$

and can be expanded in orders of the interaction coefficients, $\hat{\kappa}(t) = \sum_n \hat{\kappa}_n(t)$. We emphasize that $\hat{\kappa}(t)$ depends on *both* the stochastic process $b(t)$ and the coupling coefficient to the vacuum field Γ . For sufficiently *weak coupling* to both the classical and quantum baths, we truncate the TCL generator expansion at the second order. Accordingly, we have $\hat{\kappa}_1(t) = E_1(\hat{1})$, and $\hat{\kappa}_2(t) = E_1(\hat{1}, \hat{2}) - E_1(\hat{1})E_0(\hat{1})$. Provided that $\text{Tr}_B[\rho_B H_{\Lambda\text{-vac}}(t)] = 0$, we can take $E_1(\hat{1}) = 0$ [18] (since that leads to $\hat{P}\hat{L}(t)\hat{P} = 0$). This leaves $\hat{\kappa}_2(t)$ as the only non-zero contribution, resulting in the second-order TCL ME

$$\dot{\sigma}_{\text{av}}(t) = \int_0^t ds \mathbb{E}\{\hat{P}\hat{L}(t)\hat{L}(s)\hat{P}\} \sigma_{\text{av}}(t).$$

Finally, by tracing over the quantum bath, we obtain the desired TCL ME for the Λ system alone, namely,

$$\dot{\rho}_{\text{av}}(t) = - \int_0^t ds \text{Tr}_B \mathbb{E} \left\{ [\tilde{H}_{\text{int}}(t), [\tilde{H}_{\text{int}}(s), \rho_{\text{av}}(t) \otimes \rho_B]] \right\},$$

where $\rho_{\text{av}}(t) \equiv \text{Tr}_B\sigma_{\text{av}}(t)$ is the reduced density matrix of the Λ system. Hereafter, we omit the subscript “av” for notational convenience.

By tailoring the above derivation more specifically to our system, the relevant interaction picture is $\tilde{H}_{\text{int}}(t) = \tilde{H}_{\text{drive}}(t) + \tilde{H}_c[b(t)] + \tilde{H}_{\Lambda\text{-vac}}(t)$, with

$$\tilde{H}_c[b(t)] = e^{iH_{\Lambda}^0 t} H_c(t) e^{-iH_{\Lambda}^0 t} = H_c[b(t)] = \gamma_e b(t) Z_{12},$$

and $Z_{12} \equiv |1\rangle\langle 1| - |2\rangle\langle 2|$. We thus easily arrive at

$$\dot{\rho}(t) = -i[H_{\text{drive}}(t), \rho(t)] + R_q[\rho(t)] + R_c[\rho(t)], \quad (13)$$

where R_q is the Lindblad dissipator already specified in Eqs.(8)–(9), whereas

$$R_c[\rho(t)] = -\gamma_e^2 \alpha(t) [Z_{12}^2 \rho(t) + \rho(t) Z_{12}^2 - 2Z_{12}\rho(t)Z_{12}]$$

is the time-local dissipator accounting for the additional

spin-bath noise. Here, the time-dependent strength parameter is given by

$$\alpha(t) \equiv \int_0^t ds C(t-s) = 2 \int_0^\infty d\omega S(\omega) \frac{\sin \omega t}{\omega}, \quad (14)$$

in terms of the noise correlation function $C(t)$ of Eq. (3) and the corresponding noise spectral density, determined by the Fourier transform

$$S(\omega) = \frac{1}{2\pi} \int_{-\infty}^{+\infty} d\tau C(\tau) e^{-i\omega\tau}.$$

Physically, the noise parameter $\alpha(t)$ in the ME is the only term that carries information about the history of the stochastic magnetic field, consistent with the fact that no Markovian assumption is involved in the TCL ME. Similar to Eq.(10), Eq.(13) can still be cast as a linear system of coupled differential equations,

$$\dot{\vec{\rho}} = \hat{A}'(t)\vec{\rho}, \quad \vec{\rho} \equiv (\rho_{00}, \rho_{01}, \dots, \rho_{22}), \quad (15)$$

in terms of a new superoperator matrix $\hat{A}'(t)$. However, the dynamical system is now *time-varying* in general, due to the time dependence encoded in $\alpha(t)$, which in turn stems from the colored spectrum. Characterizing the steady states and their stability becomes a significantly less straightforward problem [41], which is beyond our present scope. As an illustration of the influence that bath properties may have on the transient dynamics, we showcase in Fig.(2) the dynamics of the excited state population obtained by solving Eq.(15) for an exponentially decaying correlation function, $C(t) = c_0^2 \exp(-t/\tau_c)$, with $\gamma_e c_0 = 1\text{MHz}$ [42]. We contrast a fast ($\tau_c = 0.01\mu\text{s}$) vs. a slow ($\tau_c = 5\mu\text{s}$) bath, showing how this results in appreciably different profiles over a given observation window.

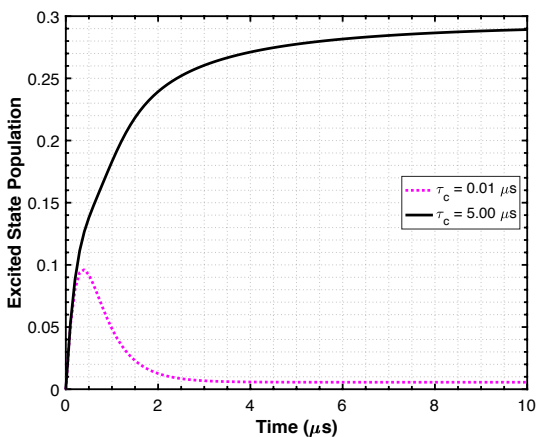


FIG. 2. (Color online) Excited-state population as a function of time for fast ($\tau_c = 0.01\mu\text{s}$, hence $\tau_2 = 100\mu\text{s}$) vs. slow ($\tau_c = 5\mu\text{s}$, hence $\tau_2 = 0.2\mu\text{s}$) stochastic baths. Parameter values are as follows: $\Omega_1 = \Omega_2 = 46\text{MHz}$, $\Gamma = 7\text{MHz}$, and $\delta = 0$. Fast oscillations have been removed for clarity.

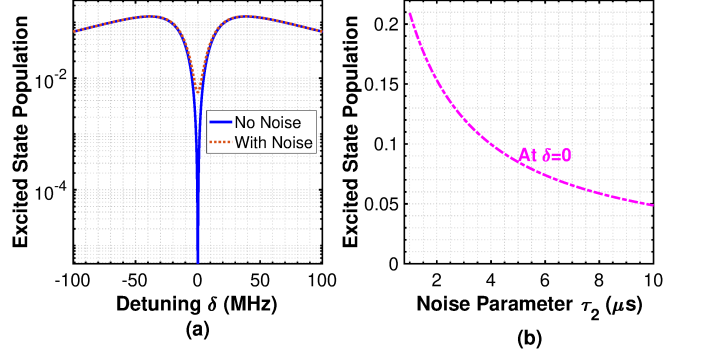


FIG. 3. (Color online) (a) Excited-state population of the Λ system versus the two-photon detuning of the two lasers; the second laser detuning is taken to be $\delta_2 = 0$. The depth of the CPT dip depends on the value of the noise parameter characterizing the classical bath. (b) Excited-state population as a function of $\tau_2 = 1/(\gamma_e^2 \alpha)$ at the CPT dip ($\delta = 0$). The values for the experimental parameters are motivated by [32] and taken to be $\Gamma = 7\text{MHz}$, $\Omega_1 = \Omega_2 = 46\text{MHz}$.

Since our main focus is CPT, which is an equilibrium phenomenon, the steady state will be seen in the long-time (effectively Markovian) limit, whereby

$$\alpha(t) = \int_0^t d\tau C(\tau) \approx \int_0^\infty d\tau C(\tau) \equiv \alpha t = S(0)t, \quad t \gg \tau_c.$$

This integral is often encountered when calculating the decoherence time for a two-level system in the presence of Gaussian dephasing [18], as $T_2^{-1} = \gamma_e^2 \alpha$. More generally, α may be related to the fastest decoherence timescale, which is the timescale over which $\rho(t)$ changes appreciably due to the coupling to the bath [43], denoted by $\tau_2 \equiv (\gamma_e^2 \alpha)^{-1}$ for our three-level system.

IV. APPLICATIONS

In this section, we illustrate how the theoretical description of CPT dynamics developed so far may be applied to two applications of independent interest.

A. Parametric noise estimation

First, by determining the steady-state solution of the ME Eq.(13), the equilibrium excited-state population may be studied as a function of relevant parameters, in particular, the detuning. In Fig.(3a), representative results are shown for CPT dynamics with and without the presence of the spin-bath noise. Notably, in the noisy case, the excited-state population no longer vanishes; rather, the characteristic CPT dip has a finite height from zero. The depth of this dip depends on the value of the noise parameter α . This is caused by the fluctuating magnetic field randomly shifting the two ground

states of the Λ system, and spoiling the destructive interference condition necessary for CPT. Interestingly, a similar steady-state behavior of driven Λ systems was reported in [44] in the presence of an incoherent optical pumping between only one of the ground states and the excited state. Likewise, including the decoherence of the ground states would also lead to a similar effect [45]. These effects will play a negligible role (if any) in the CPT setting we consider. On the one hand, no optical pumping is present in our scheme. On the other hand, the effect reported in [45] (where the ground-state decoherence time ranges from μ s to ms depending on the ^{13}C -to- ^{12}C ratio) is negligible due to the relatively fast equilibration time of the Λ system in the NV center [46].

In Fig.(3b), we present the dependence of the height of the CPT dip on the noise parameter for the special case of an exponentially decaying correlation function as considered before. Fig.(3b) allows us to infer the value of τ_2 (equivalently, α) given the CPT simulation data in Fig.(3a) and any *a priori* model for $C(\tau)$. This ability to determine α from an experimentally accessible quantity (the noisy CPT photon count) without resorting to multiple experimental set-ups may be especially advantageous in practice.

B. Qubit state preparation

State initialization of a Λ system in an arbitrary superposition of its ground states has been studied [7], with application in optically controlled solid-state spin-based quantum devices. This is accomplished by properly tuning the Rabi frequencies Ω_1, Ω_2 , as well as the phase difference $\phi_1 - \phi_2$ between the two driving fields, and using CPT to initialize the system in the dark state

$$|d\rangle = \cos\theta|1\rangle - e^{i\phi}\sin\theta|2\rangle, \quad (16)$$

where $\tan\theta = \Omega_1/\Omega_2$ and $\phi = \phi_1 - \phi_2$. The dark state is reached when the laser frequencies ω_1, ω_2 are completely in tune with the transition frequencies of the Λ system. Due to the spin-bath noise, the steady-state solution of the ME Eq.(13) will not exactly be a dark state; hence we look for its fidelity with respect to $|d\rangle$. This fidelity is a function of the experimental parameters Ω_1, Ω_2 and the noise parameter τ_2

$$f(\Omega_1, \Omega_2, \tau_2) \equiv F(\rho^{\text{eq}}, |d\rangle\langle d|) = \langle d|\rho^{\text{eq}}|d\rangle. \quad (17)$$

We assume for simplicity that $\phi = 0$ (recall that the noiseless limit corresponds to $\tau_2 \rightarrow \infty$). Since the Rabi ratio Ω_1/Ω_2 determines the dark state in Eq.(16) when $\phi = 0$, we write the fidelity in a more convenient form

$$f(\Omega_1, \Omega_2, \tau_2) = g(\Omega_1/\Omega_2, \Omega_2, \tau_2). \quad (18)$$

where g is a function that depends on Ω_1 only through the Rabi ratio Ω_1/Ω_2 .

Fig.(4a) shows the range of possible target dark states

with different Rabi ratios when the parameters Ω_2 and τ_2 are fixed. A certain threshold on the fidelity (e.g. $F > 0.98$) should be demanded for a state preparation to be successful. The fidelity plot has a dip at around the Rabi ratio $\Omega_1/\Omega_2 = 1$, corresponding to the dark state $|d\rangle = (|1\rangle - |2\rangle)/\sqrt{2}$. This is explicitly shown in the Appendix. Briefly, the dark state (which is decoupled from the bright state when no spin bath is present) gets coupled to the bright state $|b\rangle$, mediated by the fluctuating magnetic field $b(t)$. The coupling constant is given by $(\sin 2\theta)\gamma_e$ which is maximized when $\theta = \pi/4$, corresponding to $\Omega_1/\Omega_2 = 1$. Since $|b\rangle$ is coupled to the excited state, this will reduce the fidelity of the target state.

Next, we consider a fixed target dark state (i.e. a fixed Rabi ratio in Eq. (18)). Fig. (4b) shows the fidelity as a function of Ω_2 for a fixed Rabi ratio and noise parameter. We see that the fidelity quickly saturates with increasing Ω_2 . This is important because lasers in practice have a finite spectrum width around the desired frequency ω . In the presence of other excited states, this might lead to undesired excitation that takes the electrons out of the Λ system (the probability of which is proportional to the matter-field coupling, i.e., the Rabi frequency). Hence, Fig.(4b) shows that one should pick the smallest Ω_2 for which the fidelity of the target state saturates. For the specific Λ system under consideration, the undesired excitation to the next allowed level in the NV center (which is A_1) can be ignored because the energy difference between the excited states A_1 and A_2 is about 3GHz, whereas in practice the driving laser frequencies can get to the desired transition energies within an uncertainty of few tens of MHz.

Finally, Fig.(4c) shows the fidelity as a function of the noise parameter τ_2 for fixed Rabi frequencies Ω_1, Ω_2 . For values of $\tau_2 < 400\mu\text{s}$ (within the given values of other parameters), the CPT method of state initialization [7] fails to accumulate sufficient fidelity for certain target states, e.g., $F < 0.98$ for $\tau_2 = 300\mu\text{s}$ when initializing at $\Omega_1/\Omega_2 = 1$. Therefore, the decision to use the CPT method for state initialization should be accompanied by the knowledge of the noise parameter τ_2 to have a sense of the resulting state fidelity. This is accomplished by Figs. (3a, 3b) of our results.

V. CONCLUSION

We have analyzed the CPT phenomenon in the presence of a classical weakly coupled noise environment, on top of quantum vacuum noise. We have derived a TCL ME for the reduced dynamics of the driven Λ system and showed that the equilibrium state has a non-zero excited state population. We find a one-to-one correspondence between the height of the CPT dip and the value of the unknown noise parameter, allowing for experimental determination of the noise. In the presence of other experimental techniques to find environment correlation times,

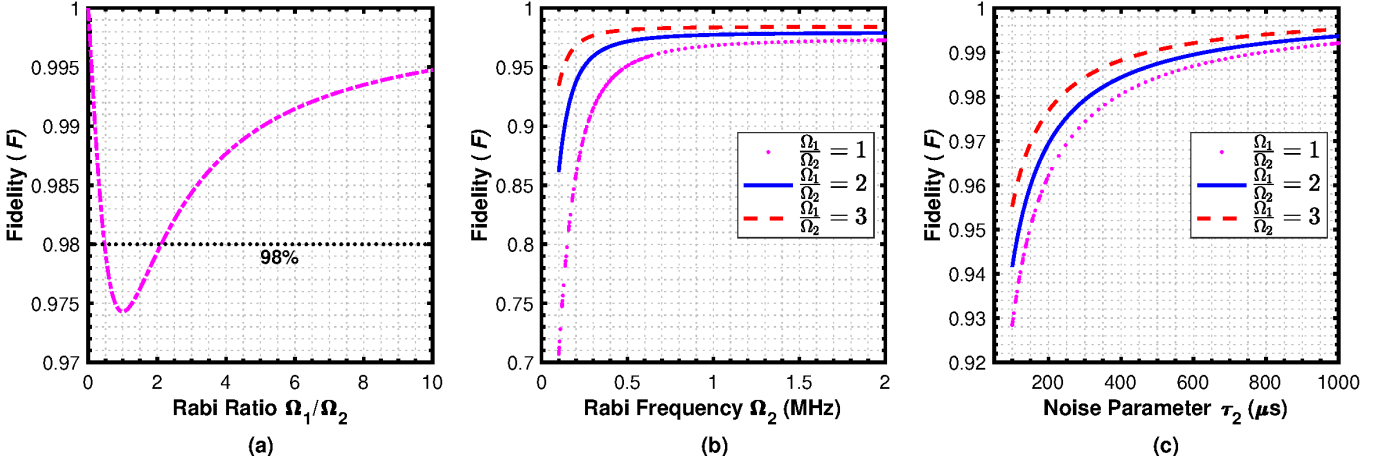


FIG. 4. (Color online) (a) The fidelity of the initialized state as a function of the Rabi ratio for a fixed $\Omega_2 = 10\text{MHz}$ and noise parameter $\tau_2 = 300\mu\text{s}$. The dip is associated with maximum coupling between the dark and bright states. (b) The fidelity of the initialized state as a function of Ω_2 for a fixed Rabi ratio and noise parameter $\tau_2 = 300\mu\text{s}$. (c) The fidelity of the initialized state as a function of noise parameter τ_2 for a fixed $\Omega_2 = 10\text{MHz}$ and Rabi ratio. Unit fidelity implies that the initialization is at the target dark state. The vacuum decay rate in all three plots is fixed at $\Gamma = 1\text{MHz}$.

the parameter estimation technique using CPT can be implemented to infer further unknown parameters of the noise model. We apply this knowledge to the problem of dissipative qubit state initialization and show that the target states prepared this way vary in fidelity.

Future efforts will be directed towards employing this noise parameter estimation method to monitor an environment with non-stationary noise. Consequently, this provides additional corrective information for the state of a nearby qubit against noise where quantum control can be applied in a feedback loop to maintain high fidelity of the qubit state.

ACKNOWLEDGEMENT

A.D., N.M., P.B., and N.B. would all like to dedicate this paper to the memory of their advisor, Jonathan P. Dowling; may he rest in peace. We would like to acknowledge Lorenza Viola and Leigh M. Norris for their guidance and support throughout the project as well as their contribution in the theoretical development of the paper. We would also like to thank Hailin Wang, Shu-Hao Wu, and Ethan Turner for useful discussions. A.D. would like to thank Lorenza Viola for her hospitality during his visit to Dartmouth College. A.D. would also like to thank Mark M. Wilde, Lior Cohen, and Hwang Lee for suggestions and comments. This work was supported by the U.S. Army Research Office through the U.S. MURI Grant No. W911NF-18-1-0218.

Appendix A: Stochastic Hamiltonian in the dark and bright state basis

Here we derive the Hamiltonian of a driven Λ system in the dark-bright-common (dbc) basis [47]. First, we write the Λ system Hamiltonian $H(t) = \hat{H}_\Lambda^0 + H_{\text{drive}}(t) + H_c[b(t)]$ in the presence of the stochastic bath as

$$\begin{aligned} H(t) = & \sum_{n=0,1,2} \omega_n P_{nn} - \gamma_e b(t)(P_{11} - P_{22}) \\ & + \frac{\Omega_1}{2}(P_{10}e^{-i(\omega_{L1}t+\phi_1)} + P_{01}e^{i(\omega_{L1}t+\phi_1)}) \\ & + \frac{\Omega_2}{2}(P_{20}e^{-i(\omega_{L2}t+\phi_2)} + P_{02}e^{i(\omega_{L2}t+\phi_2)}), \end{aligned}$$

where $P_{ij} = |i\rangle\langle j|$ are one-dimensional projectors. Next, we transform the wavefunction using the unitary

$$U_\Lambda(t) = e^{i\sum_{n=0,1,2}\omega_n P_{nn}t} \Rightarrow |\Phi(t)\rangle = U_\Lambda(t)|\Psi(t)\rangle,$$

so that the new wavefunction satisfies

$$\begin{aligned} i\partial_t|\Phi(t)\rangle &= i(\partial_t U_\Lambda(t))|\Psi(t)\rangle + U_\Lambda(t)(i\partial_t|\Psi(t)\rangle) \\ &= H_{\text{eff}}(t)|\Phi(t)\rangle, \end{aligned}$$

with the effective Hamiltonian given by

$$\begin{aligned} H_{\text{eff}}(t) = & -\gamma_e b(t)(\hat{P}_{11} - \hat{P}_{22}) + \frac{\Omega_1}{2}\hat{P}_{10}e^{-i\phi_1} \\ & + \frac{\Omega_2}{2}\hat{P}_{20}e^{-i\phi_2} + \text{H.c.} \quad (\text{A1}) \end{aligned}$$

Notice that we used the rotating basis $|\hat{1}(t)\rangle = e^{-i(\omega_{10}-\omega_{L1})t}|1\rangle$, $|\hat{2}(t)\rangle = e^{-i(\omega_{20}-\omega_{L2})t}|2\rangle$, and $|\hat{0}\rangle = |0\rangle$ to define the new projectors \hat{P}_{ij} (also note that $\hat{P}_{ii} = P_{ii}$).

The next step is to move to the dbc-basis, that is,

$$\begin{aligned} |c\rangle &= |\hat{0}\rangle, \\ |d\rangle &= e^{i\phi_2} \cos \theta |\hat{1}\rangle - e^{i\phi_1} \sin \theta |\hat{2}\rangle, \\ |b\rangle &= e^{-i\phi_1} \sin \theta |\hat{1}\rangle + e^{-i\phi_2} \cos \theta |\hat{2}\rangle, \end{aligned}$$

where, as in the main text, $\tan \theta = \Omega_1/\Omega_2$.

We now show that, in the absence of the classical noise $b(t)$, the Λ system can be thought of as a single decoupled state $|d\rangle$ and an effective driven two-level system given by the other two states ($|b\rangle$ and $|c\rangle$), with an effective Rabi frequency of $\Omega = \sqrt{\Omega_1^2 + \Omega_2^2}$. To start, we write

$$\begin{aligned} |\hat{1}\rangle &= e^{-i\phi_2} \cos \theta |d\rangle + e^{i\phi_1} \sin \theta |b\rangle, \\ |\hat{2}\rangle &= -e^{-i\phi_1} \sin \theta |d\rangle + e^{i\phi_2} \cos \theta |b\rangle, \end{aligned}$$

which gives

$$\begin{aligned} \hat{P}_{10} &= e^{-i\phi_2} \cos \theta P_{dc} + e^{i\phi_1} \sin \theta P_{bc}, \\ \hat{P}_{20} &= -e^{-i\phi_1} \sin \theta P_{dc} + e^{i\phi_2} \cos \theta P_{bc}. \end{aligned}$$

Substituting into Eq.(A1), we find $\Omega(P_{bc} + P_{cb})/2$ for the drive contribution, and the dark state is decoupled from the other two states, as claimed. After including the stochastic contribution of Eq.(A1) and using the relationships

$$\begin{aligned} P_{11} &= \cos^2 \theta P_{dd} + \sin^2 \theta P_{bb} \\ &\quad + \sin \theta \cos \theta (e^{-i(\phi_1+\phi_2)} P_{db} + \text{H.c.}), \\ P_{22} &= \sin^2 \theta P_{dd} + \cos^2 \theta P_{bb} \\ &\quad - \sin \theta \cos \theta (e^{-i(\phi_1+\phi_2)} P_{db} + \text{H.c.}), \end{aligned} \quad (\text{A2})$$

we find

$$\begin{aligned} P_{11} - P_{22} &= \cos 2\theta (P_{dd} - P_{bb}) \\ &\quad + \sin 2\theta (e^{-i(\phi_1+\phi_2)} P_{db} + e^{i(\phi_1+\phi_2)} P_{bd}). \end{aligned}$$

Therefore, the effective Hamiltonian finally reads

$$\begin{aligned} H_{\text{eff}}(t) &= -\gamma_e \cos 2\theta b(t) (P_{dd} - P_{bb}) \\ &\quad - \gamma_e \sin 2\theta b(t) (e^{-i(\phi_1+\phi_2)} P_{db} + e^{i(\phi_1+\phi_2)} P_{bd}) \\ &\quad + \frac{\Omega}{2} (P_{bc} + P_{cb}), \end{aligned}$$

where the first term describes the coupling of the dark and bright states to the stochastic magnetic field $b(t)$ with a strength that depends on the ratio of the two Rabi frequencies via $\cos 2\theta$. The second term describes a coupling between the dark and bright states mediated by the stochastic magnetic field, with a strength that is also determined by the the ratio of the two Rabi frequencies via $\sin 2\theta$. Finally, the term in the last line is the well known coupling between the bright and common states (which does not include the dark state).

When $\sin 2\theta = 0$, we expect the steady-state solution of the ME given in Eq.(13) of the main text to have the highest fidelity because the dark and bright states are uncoupled for $\sin 2\theta = 0$. This is the case when $\theta = 0$ (i.e., $\Omega_1 = 0$) or $\theta = \frac{\pi}{2}$ (i.e., $\Omega_2 = 0$). On the other hand, the coupling between the dark and bright states is maximized (and hence the fidelity of the steady state is minimized) when $\sin 2\theta = 1$ (i.e., $\theta = \frac{\pi}{4}$), which corresponds to $\Omega_1 = \Omega_2$. This explains the dip in Fig.(4a).

[1] G. Alzetta. Induced transparency. *Phys. Tod.*, 50(7):36–42, 1997.

[2] Marlan O Scully and M Suhail Zubairy. Quantum optics. *Cambridge University Press, Cambridge, UK*, 1997.

[3] Michael Fleischhauer, Atac Imamoglu, and Jonathan P Marangos. Electromagnetically induced transparency: Optics in coherent media. *Rev. Mod. Phys.*, 77:633, 2005.

[4] K Bergmann, H Theuer, and BW Shore. Coherent population transfer among quantum states of atoms and molecules. *Rev. Mod. Phys.*, 70:1003, 1998.

[5] Florian Hilser and Guido Burkard. All-optical control of the spin state in the nv- center in diamond. *Phys. Rev. B*, 86(12):125204, 2012.

[6] Francesco Ticozzi, Riccardo Lucchese, Paola Cappellaro, and Lorenza Viola. Hamiltonian control of quantum dynamical semigroups: Stabilization and convergence speed. *IEEE Trans. Autom. Control*, 57:1931–1944, 2012.

[7] Christopher G Yale, Bob B Buckley, David J Christle, Guido Burkard, F Joseph Heremans, Lee C Bassett, and David D Awschalom. All-optical control of a solid-state spin using coherent dark states. *Proc. Nat. Acad. Sciences*, 110:7595–7600, 2013.

[8] Benjamin Pingault, Jonas N Becker, Carsten HH Schulte, Carsten Arend, Christian Hepp, Tillmann Godde, Alexander I Tartakovskii, Matthew Markham, Christoph Becher, and Mete Atatüre. All-optical formation of coherent dark states of silicon-vacancy spins in diamond. *Phys. Rev. Lett.*, 113(26):263601, 2014.

[9] Yiwen Chu, Matthew Markham, Daniel J Twitchen, and Mikhail D Lukin. All-optical control of a single electron spin in diamond. *Phys. Rev. A*, 91:021801, 2015.

[10] Zheng-Yang Zhou, Mi Chen, Lian-Ao Wu, Ting Yu, and J Q You. Dark state with counter-rotating dissipative channels. *Sci. Rep.*, 7:1–11, 2017.

[11] Charles Santori, David Fattal, Sean M Spillane, Marco Fiorentino, Raymond G Beausoleil, et al. Coherent population trapping in diamond nv centers at zero magnetic field. *Opt. Express*, 14(17):7986–7994, 2006.

[12] Charles Santori, Philippe Tamarat, Philipp Neumann, Jörg Wrachtrup, Fattal, et al. Coherent population trapping of single spins in diamond under optical excitation. *Phys. Rev. Lett.*, 97:247401, 2006.

[13] D Andrew Golter, Khodadad N Dinyari, and Hailin Wang. Nuclear-spin-dependent coherent population trapping of single nitrogen-vacancy centers in diamond. *Phys.*

Rev. A, 87:035801, 2013.

[14] P Jamonneau, G Hétet, A Dréau, J-F Roch, and V Jacques. Coherent population trapping of a single nuclear spin under ambient conditions. *Phys. Rev. Lett.*, 116:043603, 2016.

[15] S.-H. Wu, E. Turner, and H. Wang. Continuous real-time sensing with a nitrogen vacancy center via coherent population trapping. *arXiv:2102.07212*, 2021.

[16] Jianbing Qi. Electromagnetically induced transparency in an inverted y-type four-level system. *Phys. Scripta*, 81:015402, 2009.

[17] Richard Morgan Whitley and CR Stroud Jr. Double optical resonance. *Phys. Rev. A*, 14(4):1498, 1976.

[18] Heinz-Peter Breuer and Francesco Petruccione. *The Theory of Open Quantum Systems*. Oxford University Press, Oxford, 2002.

[19] Ph Tamarat, NB Manson, JP Harrison, RL McMurtrie, A Nizovtsev, et al. Spin-flip and spin-conserving optical transitions of the nitrogen-vacancy centre in diamond. *New J. Phys.*, 10:045004, 2008.

[20] Yiwen Chu and Mikhail D Lukin. Quantum optics with nitrogen-vacancy centers in diamond. *Quantum Optics and Nanophotonics; C. Fabre, V. Sandoghdar, N. Treps, L. F. Cugliandolo, Eds.*, pages 229–270, 2015.

[21] Lilian Childress and Ronald Hanson. Diamond nv centers for quantum computing and quantum networks. *MRS Bulletin*, 38(2):134–138, 2013.

[22] Peter Christian Maurer, Georg Kucska, Christian Latta, Liang Jiang, Norman Ying Yao, et al. Room-temperature quantum bit memory exceeding one second. *Science*, 336(6086):1283–1286, 2012.

[23] Marcus W Doherty, Neil B Manson, Paul Delaney, Fedor Jelezko, Jörg Wrachtrup, and Lloyd CL Hollenberg. The nitrogen-vacancy colour centre in diamond. *Phys. Rep.*, 528(1):1–45, 2013.

[24] T A Kennedy, F T Charnock, J S Colton, J E Butler, R C Linares, and P J Doering. Single-qubit operations with the nitrogen-vacancy center in diamond. *Phys. Status Solidi (b)*, 233:416–426, 2002.

[25] Hannes Bernien, Bas Hensen, Wolfgang Pfaff, Gerwin Koolstra, Machiel S Blok, et al. Heralded entanglement between solid-state qubits separated by three metres. *Nature*, 497:86–90, 2013.

[26] Sunil K Mishra, L Chotorlishvili, ARP Rau, and J Bevkardar. Three-level spin system under decoherence-minimizing driving fields: Application to nitrogen-vacancy spin dynamics. *Phys. Rev. A*, 90(3):033817, 2014.

[27] N B Manson, J P Harrison, and M J Sellars. Nitrogen-vacancy center in diamond: Model of the electronic structure and associated dynamics. *Phys. Rev. B*, 74:104303, 2006.

[28] Jeronimo R Maze, Adam Gali, Emre Togan, Yiwen Chu, Alexei Trifonov, Efthimios Kaxiras, and Mikhail D Lukin. Properties of nitrogen-vacancy centers in diamond: the group theoretic approach. *New J. Phys.*, 13:025025, 2011.

[29] Marcus W Doherty, Neil B Manson, Paul Delaney, and Lloyd C L Hollenberg. The negatively charged nitrogen-vacancy centre in diamond: the electronic solution. *New J. Phys.*, 13:025019, 2011.

[30] Ian Hincks, Christopher Granade, and David G Cory. Statistical inference with quantum measurements: methodologies for nitrogen vacancy centers in diamond. *New J. Phys.*, 20:013022, 2018.

[31] Emre Togan, Yiwen Chu, Alexei S Trifonov, Liang Jiang, Jeronimo Maze, et al. Quantum entanglement between an optical photon and a solid-state spin qubit. *Nature*, 466:730–734, 2010.

[32] D Andrew Golter and Hailin Wang. Optically driven rabi oscillations and adiabatic passage of single electron spins in diamond. *Phys. Rev. Lett.*, 112(11):116403, 2014.

[33] Nan Zhao, Sai-Wah Ho, and Ren-Bao Liu. Decoherence and dynamical decoupling control of nitrogen vacancy center electron spins in nuclear spin baths. *Phys. Rev. B*, 85:115303, 2012.

[34] Iyyanki V Jyotsna and G S Agarwal. Coherent population trapping at low light levels. *Phys. Rev. A*, 52:3147, 1995.

[35] Ennio Arimondo. V coherent population trapping in laser spectroscopy. *Progr. Opt.*, 35:257–354, 1996.

[36] S. G. Schirmer and Xiaoting Wang. Stabilizing open quantum systems by markovian reservoir engineering. *Phys. Rev. A*, 81:062306, 2010.

[37] Ryogo Kubo. Stochastic liouville equations. *J. Math. Phys.*, 4:174–183, 1963.

[38] Nicolaas Godfried Van Kampen. *Stochastic Processes in Physics and Chemistry*, volume 1. Elsevier, Amsterdam, 1992.

[39] Mizuhiko Saeki. Stochastic liouville equation for weakly driven system. i: —tcl equation and its application to a quantal oscillator—. *Progr. Theor. Phys.*, 79(2):396–415, 1988.

[40] NG Van Kampen. A cumulant expansion for stochastic linear differential equations. ii. *Physica*, 74:239–247, 1974.

[41] Achim Ilchmann, David H. Owens, and D. Prätzel-Wolters. Sufficient conditions for stability of linear time-varying systems. *Syst. Control Lett.*, 9:157, 1987.

[42] G. De Lange, Z. H. Wang, D. Riste, V. V. Dobrovitski, and R. Hanson. Universal dynamical decoupling of a single solid-state spin from a spin bath. *Science*, 330(6000):60–63, 2010.

[43] Evgeny Mognunov and Daniel A. Lidar. Completely positive master equation for arbitrary driving and small level spacing. *Quantum*, 4:227, 2020.

[44] M Blaauboer. Steady-state behavior in atomic three-level λ and ladder systems with incoherent population pumping. *Phys. Rev. A*, 55(3):2459, 1997.

[45] Xiaodong Xu, Bo Sun, Paul R Berman, Duncan G Steel, Allan S Bracker, Dan Gammon, and LJ Sham. Coherent population trapping of an electron spin in a single negatively charged quantum dot. *Nat. Phys.*, (9):692–695, 2008.

[46] Ignas Lekavicius, D Andrew Golter, Thein Oo, and Hailin Wang. Transfer of phase information between microwave and optical fields via an electron spin. *Phys. Rev. Lett.*, 119(6):063601, 2017.

[47] R N Shakhmuratov, Joseph Odeurs, Romain Coussemant, and A Szabo. Dark and bright states of the coherently excited three-level atom. *Laser Phys.*, 14:39–50, 2004.